• **Basic Research** •

Inhibition of retinal angiogenesis by gold nanoparticles *via* inducing autophagy

Ni Shen[1,2], Rui Zhang[2], Hao-Rui Zhang[2,3], Hao-Yang Luo[4], Wei Shen[2], Xin Gao[2], Da-Zhi Guo[5], Jie Shen[1]

[1]Department of Ophthalmology, Shanghai Renji Hospital, Shanghai Jiao Tong University School of Medicine, Shanghai 200127, China

[2]Department of Ophthalmology, Changhai Hospital, the Second Military Medical Univerisity, Shanghai 200433, China

[3]Company 6 of Basic Medical School, the Second Military Medical University, Shanghai 200433, China

[4]School of Life Science, Fudan University, Shanghai 200082, China

[5]Department of Hyperbaric Oxygen, Navy General Hospital, Beijing 100037, China

Co-first authors: Ni Shen, Rui Zhang and Hao-Rui Zhang
Correspondence to: Jie Shen. Department of Ophthalmology, Shanghai Renji Hospital, Shanghai Jiao Tong University School of Medicine, Shanghai 200127, China. jshenrenji@163.com
Received: 2018-05-18   Accepted: 2018-06-26

Abstract
● **AIM: To investigate the effect of gold nanoparticles on retinal angiogenesis *in vitro* and *in vivo*, and to reveal the possible mechanism.**

● **METHODS: Seed growth method was used to synthesize gold nanoparticles (GNPs). The size, zeta potential, absorption spectrum and morphology of GNPs were identified using Malvern Nano-ZS, multimode reader (BioTek synergy2) and transmission electron microscope. Cell viability was analyzed using cell counting kit-8 method and cell growth was assessed with EdU kit. Transwell chamber was used to investigate cell migration. Tube formation method was used to assess the angiogenic property *in vitro*. Oxygen induced retinopathy (OIR) model was used to investigate the effect of GNPs on retinal angiogenesis. Confocal microscope and Western blot were used to study the possible mechanism of GNPs inhibited angiogenesis.**

● **RESULTS: The GNPs synthesized were uniform and well dispersed. GNPs of 10 μg/mL and 20 μg/mL were able to inhibit human umbilical vein endothelial cells proliferation (50% and 72% separately, *P*<0.001), migration (54% and 83% separately, *P*<0.001) and tube formation (52% and 90% separately, *P*<0.001). Further data showed that GNPs were able to improve the retinopathy in an OIR model. The possible mechanism might be that GNPs were able to induce autophagy significantly (*P*<0.05).**

● **CONCLUSION: The present study suggests that GNPs are able to inhibit retinal neovascularization *in vitro* and *in vivo*. GNPs might be a potential nanomedicine for the treatment of retinal angiogenesis.**

● **KEYWORDS:** gold nanoparticles; retinal angiogenesis; oxygen induced retinopathy; autophagy; nanomedicine

INTRODUCTION

Angiogenesis is the outgrowth of new blood vessels from the pre-existing vascular[1]. It is a strictly-controlled process which contains the growth, migration and sprouting of vascular endothelial cells[1]. In physiological conditions, angiogenesis plays an important role in development, growth, regeneration, would healing and the balance of circulation[2-3]. However, pathological angiogenesis can cause a variety of severe diseases such as tumor, retinopathy and rheum arthritis[4]. Diabetic retinopathy, age-related macular degeneration (AMD) and retinopathy of prematurity (ROP) are three major retinopathies that would lead to vision loss even blindness[5]. Vascular endothelial growth factor (VEGF) is the major growth factor that increases angiogenesis, and anti-VEGF drugs have improved the treatment of angiogenic retinopathy greatly. However, some patients can be resistant to these drugs[6]. Therefore, novel anti-angiogenic drugs need to be explored.

Due to the small size and specific physiochemical properties, gold nanoparticles (GNPs) have been well studied in bio-imaging, drug-delivery, nanomedicine and bio-sensing[7-8]. Previous investigations show that GNPs could inhibit VEGF induced endothelial cell migration *via* Akt pathway[9]. Meanwhile, GNPs could induce nanostructural reorganization of vascular endothelial growth factor receptor 2 (VEGFR2) and inhibit VEGFR2 activation to suppress angiogenesis[10-11]. These studies focus on the effect of GNPs on VEGF signaling pathway, while their effects on other molecular pathway in angiogenesis are largely unknown. It is reported that GNPs could induce autophagy in human renal proximal tubular cells and normal rat kidney cells[12-13]. Thus, it is meaningful to see whether GNPs could induce autophagy to suppress retinal angiogenesis *in vitro* and *in vivo*.

In the present investigation, we synthesized uniform GNPs and evaluated their effects on retinal neovascularization. The results showed that GNPs were able to inhibit the proliferation, migration and tube formation of endothelial cells and could suppress retinal angiogenesis *in vivo*. The possible mechanism was that GNPs were able to induce autophagy. The study highlights the potential of GNPs as therapeutic nanomedicine in treatment of angiogenesis, and provides novel insights for ocular angiogenesis therapy.

MATERIALS AND METHODS

Reagents Cetyltrimethyl ammonium bromide (CTAB), hydrogen tetrachloroaurate (III) trihydrate (HAuCl$_4$.3H$_2$O), trisodium citrate and sodium borohydride (NaBH$_4$) were purchased from Sangon Biotech. Fetal bovine serum (FBS), Dulbecco's modified Eagle medium (DMEM), Horseradish Peroxidase (HRP)-conjugated mouse and rabbit secondary antibodies were purchased from Invitrogen (Shanghai, China). EdU cell proliferation kit was purchased from RiboBio (Guangzhou, China). Cell counting kit-8 (CCK-8) reagent was obtained from Dojindo (Shanghai, China). The antibody to p62 was purchased from Abcam (Shanghai, China). Antibodies to LC3, Beclin1, autophagy-related protein 5 (ATG5) and glyceraldehyde phosphate dehydrogenase (GAPDH) were purchased from CST (Shanghai, China). Isolectin B4 reagent was obtained from Sigma-Aldrich (Shanghai, China). Matrigel Matrix, transwell chamber unite and other cell culture plates were obtained from Corning, Inc. (Shanghai, China).

Synthesis and Characterization of Gold Nanoparticles
GNPs were synthesized as previously described[14]. Briefly, 20 mL aqueous solution containing 0.25 mmol/L HAuCl$_4$ and 0.25 mmol/L trisodium citrate was prepared. Then, 0.6 mL of ice-cold 0.1 mol/L NaBH$_4$ solution was added to the solution with stirring. The particles in this solution were used as seeds. Totally 200 mL aqueous solution of 0.25 mmol/L HAuCl$_4$ and 80 mmol/L CTAB was prepared. The solution was used as a stock growth solution.

Furthermore, 7.5 mL of growth solution was mixed with 0.05 mL 0.1 mol/L ascorbic acid solution and then 2.5 mL of seed solution was added into the solution with stirring until the solution turned wine red. The nanoparticles in wine red solution were used as seeds for the growth of larger nanoparticles. And the procedure was performed another 2 times, when the color of the solution was reddish brown. Then, the reaction was stopped by centrifugation. The size and zeta potential of GNPs were determined using Malvern Nano-ZS. Transmission electron microscope (TEM; H-7650, Hitachi) was used to observe the shape of GNPs. Biotek synergy2 (Biotek) was used to determine the absorption spectrum of GNPs. Inductively coupled plasma mass spectrometry (ICP-MS, NexION 300X, PE, USA) was used to determine the concentration of GNPs.

Cell Culture Human umbilical vein endothelial cells (HUVECs) were obtained from KeyGEN BioTECH (Nangjing, China). The cells were cultured in DMEM supplemented with 10% FBS, 1% L-glutamine in a 5% CO$_2$ incubator at 37℃. When the cells grow to about 80% confluence, the cells were seeded into the corresponding plate for different experiments.

Cell Viability Assay Cell viability was assessed using CCK-8 reagent. Briefly, about 2000 cells were seeded into 96-well plate and cultured overnight. Then, the growth medium was replaced with fresh medium containing different concentrations of GNPs and cultured for another 2d. We then discarded the medium, washed the cells 2 times with phosphate buffered saline (PBS) and added 110 μL fresh medium containing 10 μL CCK-8 reagent. After incubating the sample for approximately 2h, the optical density was measured at 450 nm using Biotek synergy2 (Biotek, USA).

Cell Proliferation Assay Cell proliferation was determined using EdU regent as described previously[15]. Briefly, 1500 cells were seeded into a 96-well plate and treated with GNPs for 48h. Then the culture medium was replaced with fresh medium containing EdU regent. After incubation with EdU for 2h, the cells were fixed with 4% paraformaldehyde for half an hour. Next, the cells were washed with glycine once and washed with 0.2% Trion X-100 twice. Then, the cells were treated with Apollo fluorescent azide for half an hour. Next, the cells were washed with 0.2% Trion X-100 twice. After the cells being stained with Hoechst for 15min, the images were captured using a digital microscope (IX81, Olympus, Japan).

Cell Migration Assay Of 10^4 cells treated with GNPs for 48h were seeded into the upper side of transwell unit in culture medium containing 0.5% FBS. The 24-well plate was filled with 700 μL DMEM containing 1% FBS. And 12h later, the culture medium was dumped and the chambers were fixed with 4% paraformaldehyde for 20min. Next, cells on the upper surface of the transwell unit were completely removed using a cotton swab. Then, the chambers were stained with 0.1% Crystal violet for half an hour. After two washes with PBS, the migrated cells were captured and analyzed using a digital microscope (IX81, Olympus, Japan).

Tube Formation Assay Tube formation experiment was performed as we previous described[16]. In brief, 50 μL Matrigel was added into 96-well plate and incubated at 37℃ for half an hour for hardening. HUVEC treated with GNPs for 48h were harvested using trypsin. Then, about 2×10^4 cells in 100 μL culture medium was added into Matrigel-coated plate. Then the cells were incubated at 37℃ for 4h to form capillary structures. The tubes were then captured under a digital microscope (IX81, Olympus, Japan).

Oxygen Induced Retinopathy Mice Model C57BL/6 mice were purchased from SIPPR-BK Experimental Animal Co. (Shanghai, China). All animal experiments were conducted in

agreement with the approval of the Institutional Animal Care and Use Committee at Second Military Medical University. The oxygen induced retinopathy (OIR) model was used to analyze retinal angiogenesis. From P7 to P12, mice were exposed to 75% oxygen. Then mice were randomly assigned to control and GNPs group. The intra-vitreal injection of GNPs (0.4 μL of 1.2 μg GNPs) was delivered using a 34 G needle at P12. The control groups were injected with PBS (0.4 μL). Retinas were separated and fixed in 4% paraformaldehyde overnight at 4℃. Then the retinas were blocked in 3% bovine serum albumin (BSA) for 4h and permeabilized with 0.5% Triton X-100 for 12h at 4℃. After three washes with PBS, the retinas were stained with FITC-labelled isolectin B4 overnight at 4℃. After three washes with PBS, the retinas were placed on slides and captured using a microscope (IX81, Olympus, Japan).

Autophagy Analysis mTagRFP-MWasabi-LC3 plasmid was used to evaluate the effect of GNPs on autophagy. The lentivirus of mTagRFP-MWasabi-LC3 was packaged using Vesicular stomatitis virus-glycoprotein (VSV-G), regulator of virion expression (REV) and pMDL plasmids. mTagRFP-MWasabi-LC3 lentivirus were then used to infect cells. The infected cell were seeded into polystyrene/glass bottom cell culture dish (Nest, Shanghai, China). Furthermore, the cells were treated with different concentrations of GNPs for 48h. The cells were then fixed with 4% paraformaldehyde for 20min and stained with Hoechst for 15min. After two washes with PBS, the cells were observed with Zeiss LSM-710 confocal microscope (Zeiss, Germany).

Western Blot Assay The protein was extracted using RIPA lysis buffer containing proteinase inhibitor. About 20 μg proteins were electrophoresed and transferred to polyvinylidene fluoride (PVDF) membranes. The membranes were blocked with 5% skimmed milk for 1h at room temperature. Then the membranes were incubated with different primary antibodies at 4℃ overnight. Furthermore, the membranes were incubated with HRP-conjugated secondary antibodies at room temperature for 2h. Then, the blots were incubated with chemoluminescent substrate (Thermo Fisher Scientific, Shanghai, China) and visualized using the GeneGnome HR Image Capture System (Syngene, Frederick, MD, USA).

Statistical Analysis Prism software (GraphPad 5.0) was used to analyze all the data. Data were presented as the mean± standard deviation (SD). The differences between groups were evaluated using t-test or one-way ANOVA test. $P<0.05$ was supposed to be statistically significant.

RESULTS

Characteristics of Gold Nanoparticles GNPs were synthesized using a seed-mediated growth method. The GNPs had an average size of 26.2±2.8 nm and an average zeta potential of 24.9±1.1 mV determined by Malvern Nano-ZS (Figure 1A, 1B). The GNPs had the highest absorption at 525 nm (Figure 1C).
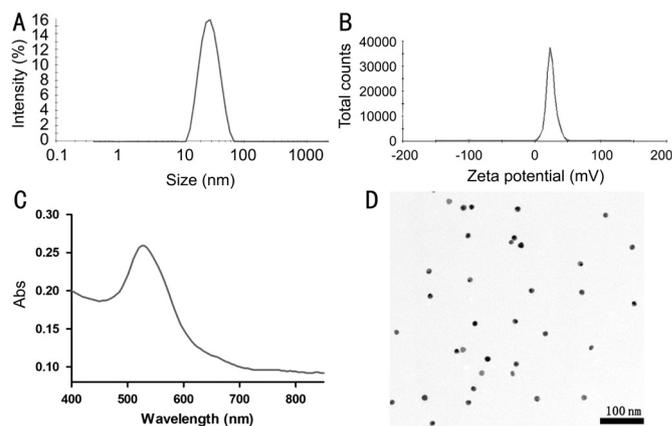

Figure 1 The characteristics of GNPs A: The size of GNPs; B: The zeta potential of GNPs; C: The absorption spectrum of GNPs; D: The morphology of GNPs determined by TEM.

The result of TEM revealed that GNPs were uniform and round nanoparticles (Figure 1D).

Inhibition of Cells Proliferation by Gold Nanoparticles In order to choose proper concentrations of GNPs, we initially evaluated the effect of GNPs on cell viability. The data showed that GNPs could reduce cell viability when the concentrations were higher than 5 μg/mL (Figure 2A). Therefore, we chose the concentration of 10 and 20 μg/mL to perform subsequent experiments.

Then, the growth of HUVEC treated with GNPs was assessed with EdU kit. Being a nucleoside analog of thymidine, EdU could be incorporated into DNA in the DNA synthesis process. Therefore, the ratio of EdU positive cells could be used to evaluate the ability of DNA replication, thus determining the proliferate rate of cells. GNPs could reduce the ration of EdU positive nuclei dose dependently compared with control group (Figure 2B). Quantitative data revealed that the EdU positive nuclei were decreased by 50% and 72% separately (Figure 2C). These results indicated that GNPs could inhibit HUVEC proliferation dose dependently.

Suppression of Cells Migration by Gold Nanoparticles Cell migration is a vital step for the sprouting of endothelial cells[17]. In order to form the vessels, the cells need to migrate to the right position. Here, the data showed that GNPs were able to inhibit HUVEC migration dose dependently (Figure 3A-3C). Quantitative result revealed that GNPs were able to suppress the migration of HUVEC by 54% and 83% separately compared with control group (Figure 3D).

Inhibition of Tube Formation by Gold Nanoparticles Tube formation of endothelial cells is another key step that participates in the process of angiogenesis[18]. Matrigel matrix is commonly used to evaluate the angiogenic properties *in vitro*, as vascular endothelial cells could attach, align and form vessel like structures. The results showed that with the treatment of GNPs the capillary-like structures were apparently impaired (Figure 4A-4C). Quantitative result revealed that
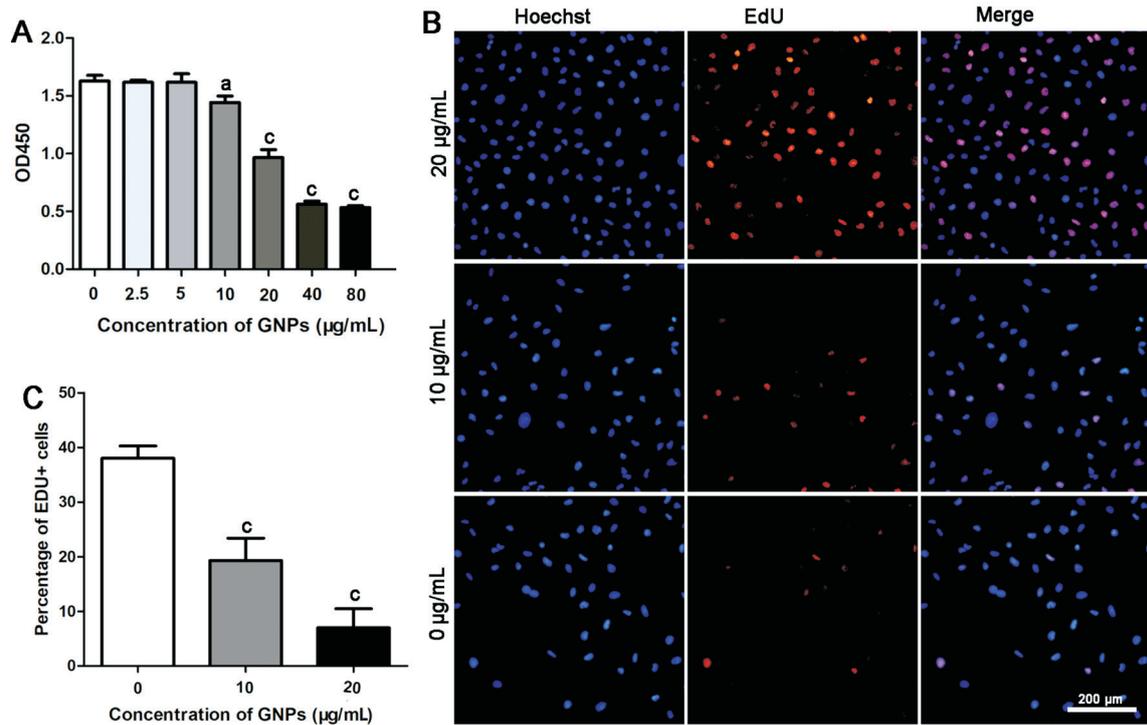
Figure 2 GNPs inhibit HUVEC proliferation A: Cell viability of different concentration of GNPs determined by CCK-8; B: Representative images of EdU assay; C: Quantitative results of EdU positive cells. Data are shown as mean±SD. $^aP<0.05$; $^cP<0.001$.
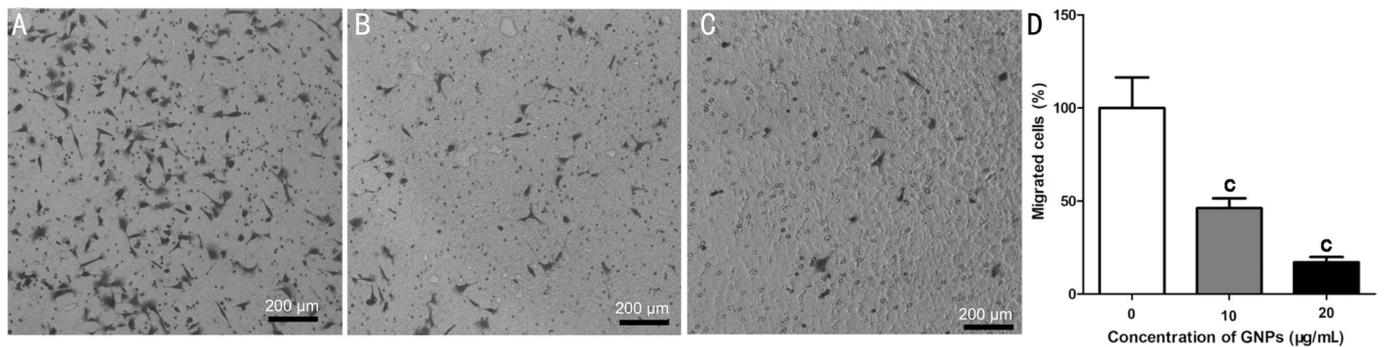

Figure 3 GNPs inhibit HUVEC migration HUVEC were treated with GNPs for 48h and then cell migration was evaluated using transwell chamber. Representative images of migrated cells of 0 μg/mL (A), 10 μg/mL (B), 20 μg/mL (C) groups; D: Quantitative data of the migrated cells. Data are shown as mean±SD. $^cP<0.001$.
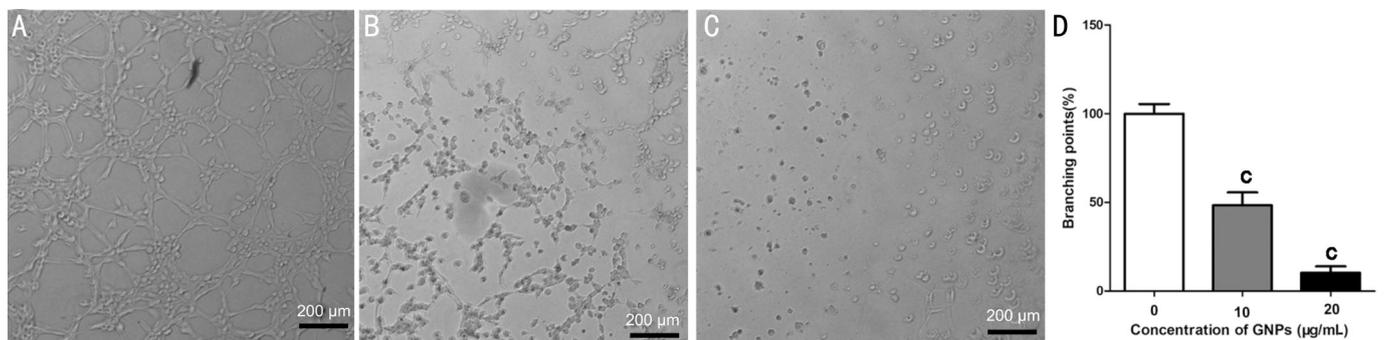

Figure 4 GNPs inhibit HUVEC tube formation HUVEC were treated with GNPs for 48h and then tube formation assay was performed using Matrigel. Representative images of tube formation in 0 μg/mL (A), 10 μg/mL (B), 20 μg/mL groups (C); D: Quantitative data of the branching points. Data are shown as mean±SD. $^cP<0.001$.

the tube formation capability was decreased by 52% and 90% separately compared with the control group.

Improvement of Oxygen Induced Retinopathy after Gold Nanoparticles Treatment The development of retinal vascular is
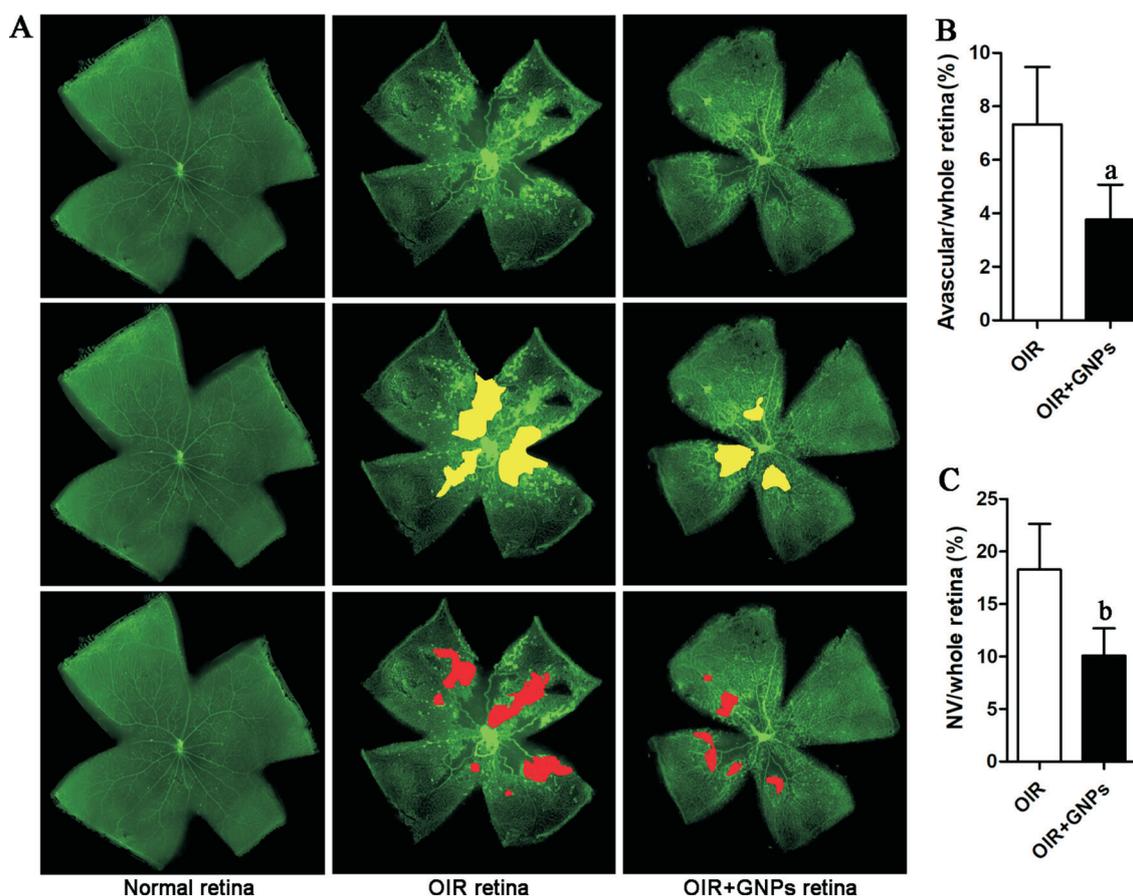
Figure 5 GNPs inhibit oxygen induced retinopathy *in vivo* A: Representative images of retinal angiogenesis stained with IB4. IB4 stained vascular vessels (green), avascular area (yellow) and neovascularization (red); B: Quantitative analysis of the avascular area; C: Quantitative analysis of the neovascularization area. Data are shown as mean±SD. [a]$P<0.05$, [b]$P<0.01$, [c]$P<0.001$.

affected by the concentration of oxygen. A higher concentration of oxygen would lead to pathological angiogenesis, which is marked by the hemorrhage, avascular area and neovascular areas[19]. As shown in Figure 5A, the vascular in normal retina is well organized and there is no avascular area and neovascular area. In the oxygen induced retinopathy group, there are many avascular areas and lots of neovascular areas. In GNPs treated group, both the avascular area and neovascular area were reduced (Figure 5B, 5C). These data suggested that GNPs exhibit good therapeutic efficiency in oxygen induced retinopathy treatment.

Induction of Autophagy by Gold Nanoparticles Autophagy is a strictly regulated process that plays an vital role in cell growth, transition and death[20]. Increasing investigations reveal that autophagy involves in the formation of angiogenesis[21-23]. In order to evaluate the effect of GNPs on autophagy, we detected the accumulation of LC3 using confocal microscopy. The results showed that the green fluorescence and red fluorescence distributed equally in the control group (Figure 6). While, in the GNPs treated group, there were lots of green dots and red dots, which indicated that GNPs could induce apparent autophagy in HUVEC.

Altered Expression of Autophagic Markers After Gold Nanoparticle Treatment To further confirm the induction

of autophagy, we used Western blot to detect the expression of autophagic markers. There are two forms of LC3 protein, LC3-I and LC3-II. LC3-II is the lapidated form of LC3-I, and is the marker of autophagy activation[24]. As was shown in Figure 7, the expression of LC3-II was increased and the expression of LC3-I was decreased with the treatment of GNPs. ATG5 and Beclin1 participate in the formation of autophagosome which is the initial process of autophagy[25]. The results showed that GNPs could increase the expression of ATG5 and Beclin1, which indicated that GNPs could induce autophagy at early stage. p62 is the marker to detect the degradation of cargo which usually degraded in the lysosome[26]. The data showed that GNPs could increase the expression of p62, which indicated that the degradation process was impaired.

DISCUSSION

Retinal pathological angiogenesis is one of the major reasons that cause severe vision loss[27]. Recently, anti-VEGF therapy has become the most effective therapeutic treatment. However, the drugs are very expensive and some patients could raise resistance to them[6]. GNPs are easily synthesized and the cost is relatively low. Meanwhile, previous reports suggest that GNPs are able to suppress angiogenesis trough VEGF signaling pathway[9-11]. Here, we investigated the effect of
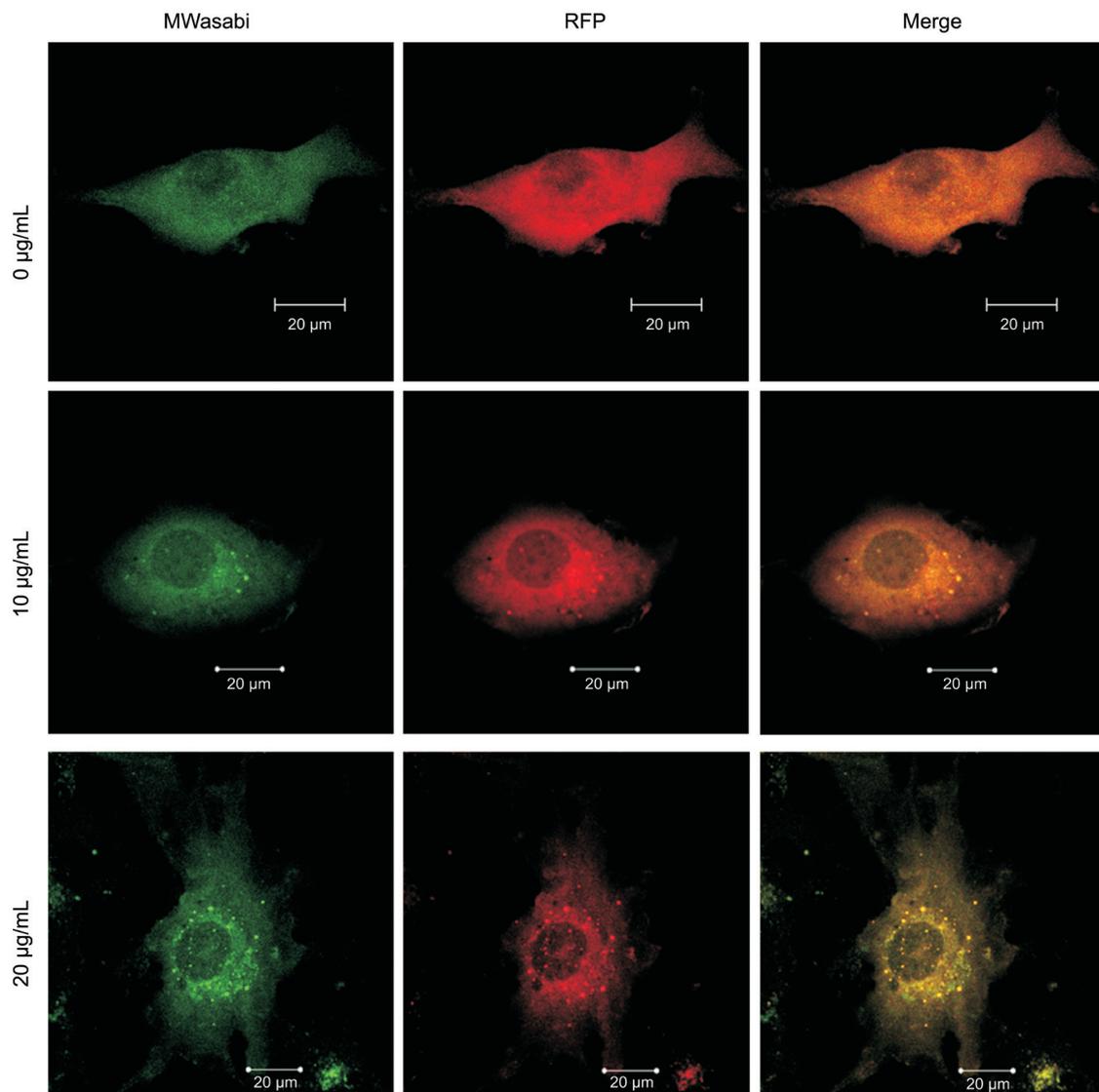
Figure 6 GNPs induce autophagy in HUVEC Confocal microscopy images of autophagic dots. The green dots indicated the initial process of autophagy and the red dots indicated the late process of autophagy.
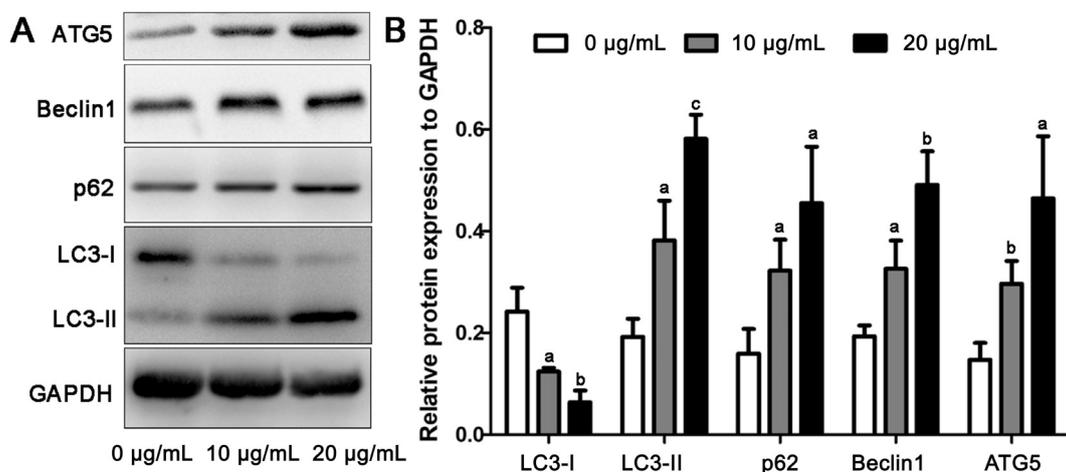

Figure 7 GNPs alter the expression of autophagic markers A: The conversion of LC3-I to LC3-II and the expression of ATG5, Beclin1 and p62 were evaluated using Western blot; B: Quantitative data of the Western blot. Data are shown as mean±SD. [a]$P<0.05$, [b]$P<0.01$, [c]$P<0.001$.

GNPs on retinal angiogenesis *in vitro* and *in vivo*, and explored the possible mechanism other than VEGF signaling pathway. The data proved that GNPs could inhibit retinal angiogenesis *via* inducing autophagy.

Autophagy is a natural, strictly-regulated and destructive metabolic process which is widely existed in eukaryotic cells[28].

Autophagy allows the cells to disassemble unnecessary and dysfunctional components orderly, and to reuse the digested nutrients[28]. There are three major process of autophagy, named the formation of autophagosome, fusion with lysosome and degradation of cargo. The relationship between autophagy and angiogenesis is complicated and up-regulated autophagy could either increase or inhibit angiogenesis[22]. Autophagy that inhibits angiogenesis usually accompanied with the impaired function of lysosomes[29-31]. The disruption of lysosomes would stop the fusion between autophagosome and lysosome, leading to autophagic cell death. ATG5 and Beclin1 are two key proteins that involves in the formation of autophagosome and autophagic cell death[25]. Our data showed that GNPs treatment could increase the expression of ATG5 and Beclin1, indicating that GNPs were able to initiate autophagy. LC3 is the well-known marker which could form stable association with the membrane of autophagosome. There are two forms, named LC3-I and LC3-II. LC3-I is usually found in the cytoplasm and LC3-II is converted from LC3-I with the modification of lipid. LC3-II is membrane-bound which involves in autophagosome membrane expansion[24]. The present study showed that there was an accumulation of GFP-LC3 dots and an increased expression of LC3-II, proving that GNPs could induce HUVEC autophagy.

p62 protein also known as sequestosome 1 is a ubiquitin-binding scaffold protein that used as a reporter of autophagy. p62 can be incorporated into the autophagosome and finally degraded with the degradation of autophagosome. Therefore, in normal autophagy, the expression of p62 usually is contrary to the expression of LC3-II[32]. However, our data showed that both LC3-II and p62 were increased with the treatment of GNPs. The reason might be that the autophagosomes were not degraded in GNPs treated cells. This was further confirmed by the confocal images that GFP-LC3 was not degraded resulting in the yellow color in the merged images. GFP-LC3 is sensitive to the acid lysosomes and green the fluorescence will quench while the red fluorescence will not. The increased activation of autophagy without degradation will result in autophagic cell death. Altogether, our data suggested that GNPs could suppress angiogenesis through inducing autophagy.

In conclusion, this study demonstrated that GNPs could inhibit angiogenesis *in vitro* and *in vivo* by inducing autophagy. The study highlights the potential of GNPs as therapeutic nanomedicine in the treatment of angiogenesis, and provides novel insights for ocular angiogenesis therapy.

ACKNOWLEDGEMENTS

Conflicts of Interest: Shen N, None; **Zhang R,** None; **Zhang HR**, None; **Luo HY,** None; **Shen W,** None; **Gao X,** None; **Guo DZ,** None; **Shen J,** None.

REFERENCES

1 Carmeliet P, Jain RK. Molecular mechanisms and clinical applications of angiogenesis. *Nature* 2011;473(7347):298-307.

2 Christiaens V, Lijnen HR. Angiogenesis and development of adipose tissue. *Mol Cell Endocrinol* 2010;318(1-2):2-9.

3 Dejana E. The role of wnt signaling in physiological and pathological angiogenesis. *Circ Res* 2010;107(8):943-952.

4 Chung AS, Ferrara N. Developmental and pathological angiogenesis. *Annu Rev Cell Dev Biol* 2011;27:563-584.

5 Rubio RG, Adamis AP. Ocular angiogenesis: vascular endothelial growth factor and other factors. *Dev Ophthalmol* 2016;55:28-37.

6 Yang S, Zhao J, Sun X. Resistance to anti-VEGF therapy in neovascular age-related macular degeneration: a comprehensive review. *Drug Des Devel Ther* 2016;10:1857-1867.

7 Li N, Zhao P, Astruc D. Anisotropic gold nanoparticles: synthesis, properties, applications, and toxicity. *Angew Chem Int Ed Engl* 2014; 53(7):1756-1789.

8 Daraee H, Eatemadi A, Abbasi E, Fekri Aval S, Kouhi M, Akbarzadeh A. Application of gold nanoparticles in biomedical and drug delivery. *Artif Cells Nanomed Biotechnol* 2016;44(1):410-422.

9 Pan Y, Wu Q, Qin L, Cai J, Du B. Gold nanoparticles inhibit VEGF165-induced migration and tube formation of endothelial cells via the Akt pathway. *Biomed Res Int* 2014;2014:418624.

10 Pan Y, Ding H, Qin L, Zhao X, Cai J, Du B. Gold nanoparticles induce nanostructural reorganization of VEGFR2 to repress angiogenesis. *J Biomed Nanotechnol* 2013;9(10):1746-1756.

11 Kim JH, Kim MH, Jo DH, Yu YS, Lee TG, Kim JH. The inhibition of retinal neovascularization by gold nanoparticles via suppression of VEGFR-2 activation. *Biomaterials* 2011;32(7):1865-1871.

12 Ma X, Wu Y, Jin S, Tian Y, Zhang X, Zhao Y, Yu L, Liang XJ. Gold nanoparticles induce autophagosome accumulation through size-dependent nanoparticle uptake and lysosome impairment. *ACS Nano* 2011;5(11):8629-8639.

13 Ding F, Li Y, Liu J, Liu L, Yu W, Wang Z, Ni H, Liu B, Chen P. Overendocytosis of gold nanoparticles increases autophagy and apoptosis in hypoxic human renal proximal tubular cells. *Int J Nanomedicine* 2014;9:4317-4330.

14 Jana NR, Gearheart L, Murphy CJ. Seeding growth for size control of 5-40 nm diameter gold nanoparticles. *Langmuir* 2001; 17(22):6782-6786.

15 Song H, Wang W, Zhao P, Qi Z, Zhao S. Cuprous oxide nanoparticles inhibit angiogenesis via down regulation of VEGFR2 expression. *Nanoscale* 2014;6(6):3206-3216.

16 Shen W, Zhu S, Qin H, Zhong M, Wu J, Zhang R, Song H. EDIL3 knockdown inhibits retinal angiogenesis through the induction of cell cycle arrest in vitro. *Mol Med Rep* 2017;16(4):4054-4060.

17 Cao J, Ehling M, März S, Seebach J, Tarbashevich K, Sixta T, Pitulescu ME, Werner AC, Flach B, Montanez E, Raz E, Adams RH, Schnittler H. Polarized actin and VE-cadherin dynamics regulate junctional remodelling and cell migration during sprouting angiogenesis. *Nat Commun* 2017;8(1):2210.

18 Rezzola S, Belleri M, Gariano G, Ribatti D, Costagliola C, Semeraro F, Presta M. In vitro and ex vivo retina angiogenesis assays. *Angiogenesis* 2014;17(3):429-442.

19 Connor KM, Krah NM, Dennison RJ, Aderman CM, Chen J, Guerin KI, Sapieha P, Stahl A, Willett KL, Smith LE. Quantification of oxygen-induced retinopathy in the mouse: a model of vessel loss, vessel regrowth and pathological angiogenesis. *Nat Protoc* 2009; 4(11):1565-1573.

20 Kimura T, Jia J, Claude-Taupin A, Kumar S, Choi SW, Gu Y, Mudd M, Dupont N, Jiang S, Peters R, Farzam F, Jain A, Lidke KA, Adams CM, Johansen T, Deretic V. Cellular and molecular mechanism for secretory autophagy. *Autophagy* 2017;13(6):1084-1085.

21 Du J, Teng RJ, Guan T, Eis A, Kaul S, Konduri GG, Shi Y. Role of autophagy in angiogenesis in aortic endothelial cells. *Am J Physiol Cell Physiol* 2012;302(2):C383-C391.

22 Liu J, Fan L, Wang H, Sun G. Autophagy, a double-edged sword in anti-angiogenesis therapy. *Med Oncol* 2016;33(1):10.

23 Ramakrishnan S, Nguyen TM, Subramanian IV, Kelekar A. Autophagy and angiogenesis inhibition. *Autophagy* 2007;3(5):512-515.

24 Klionsky DJ, Abdelmohsen K, Abe A, Abedin MJ, Abeliovich H, Acevedo Arozena A, *et al*. Guidelines for the use and interpretation of assays for monitoring autophagy. *Autophagy* 2016;12(1):1-222.

25 Mizushima N, Levine B, Cuervo AM, Klionsky DJ. Autophagy fights disease through cellular self-digestion. *Nature* 2008;451(7182):1069-1075.

26 Moscat J, Diaz-Meco MT. p62 at the crossroads of autophagy, apoptosis, and cancer. *Cell* 2009;137(6):1001-1004.

27 Li X, Carmeliet P. Targeting angiogenic metabolism in disease. *Science* 2018;359(6382):1335-1336.

28 Kroemer G. Autophagy: a druggable process that is deregulated in aging and human disease. *J Clin Invest* 2015;125(1):1-4.

29 Duan J, Yu Y, Yu Y, Li Y, Huang P, Zhou X, Peng S, Sun Z. Silica nanoparticles enhance autophagic activity, disturb endothelial cell homeostasis and impair angiogenesis. *Part Fibre Toxicol* 2014;11(1):50.

30 Kumar S, Guru S, Pathania A, Kumar A, Bhushan S, Malik F. Autophagy triggered by magnolol derivative negatively regulates angiogenesis. *Cell Death Dis* 2013;4(10):e889.

31 Wu Q, Jin R, Feng T, Liu L, Yang L, Tao Y, Anderson JM, Ai H, Li H. Iron oxide nanoparticles and induced autophagy in human monocytes. *Int J Nanomedicine* 2017;12:3993-4005.

32 Bjørkøy G, Lamark T, Pankiv S, Øvervatn A, Brech A, Johansen T. Monitoring autophagic degradation of p62/SQSTM1. *Meth Enzymol* 2009;452:181-197.